

Clock Transitions Guard Against Spin Decoherence in Singlet Fission

Sina G. Lewis,¹ Kori E. Smyser,² and Joel D. Eaves^{2, a)}

¹*Department of Physics, University of Colorado Boulder, Boulder, CO 80309, USA*

²*Department of Chemistry, University of Colorado Boulder, Boulder, CO 80309, USA*

(*Corresponding author: joel.eaves@colorado.edu)

(Dated: 24 May 2022)

Short coherence times present a primary obstacle in quantum computing and sensing applications. In atomic systems, clock transitions (CTs), formed from avoided crossings in an applied Zeeman field, can substantially increase coherence times. We show how CTs can dampen intrinsic and extrinsic sources of quantum noise in molecules. Conical intersections between two periodic potentials form CTs in electron paramagnetic resonance experiments of the spin-polarized singlet fission photoproduct. We report on a pair of CTs for a two-chromophore molecule in terms of the Zeeman field strength, molecular orientation relative to the field, and molecular geometry.

PACS numbers: 03.67.Pp,03.67.-a,82.00.00,85.65.+h,33.35.+r

^{a)}Renewable and Sustainable Energy Institute (RASEI), University of Colorado Boulder, Boulder, CO 80309, USA

I. INTRODUCTION

Singlet fission (SF), a photoconversion process where one photon creates two triplet excitons, has received a significant amount of attention in the literature.^{1,2} This is mostly due to its potential in next-generation solar cells to surpass the Shockley-Queisser limit.³ More recently, SF has also been proposed as a method for generating qubits—or more accurately “qudits”—for quantum applications at or near room temperature.^{4,5}

In time-resolved electron paramagnetic resonance (trEPR) experiments, an optical pulse prepares a two-triplet excited state with singlet multiplicity 1TT on fast, typically sub-nanosecond, timescales.^{6–10} Smyser and Eaves⁴ showed how molecular symmetries could be harnessed to direct relaxation from 1TT to specific two-triplet states with multiplicity $2S + 1$ and spin angular momentum projection quantum number M , $^{2S+1}TT_M$. With a precise initial state defined, strong-field EPR pulses can manipulate coherences between the $^{2S+1}TT_M$ states. This scheme forms the basis for quantum logic. Used in this way, SF takes advantage of state-specific relaxation in both the internal conversion ($S_0 \rightarrow S_n \rightarrow ^1TT$) and intersystem crossing ($^1TT \rightarrow ^{2S+1}TT_M$) processes to generate highly “spin-polarized” states for quantum applications, solving the so-called “state initialization” problem.^{11,12}

Decoherence is the loss of phase coherence between superpositions of different quantum states. It is a major source of noise in quantum computing, information, and sensing applications. Both *intrinsic* and *extrinsic* fluctuations contribute to decoherence. The quantum fluctuations that produce uncertainties in identical measurements on identical systems can be viewed as a source of intrinsic noise.¹³ Intrinsic noise is unavoidable in molecular systems because zero-point motions deform structure. In the condensed phase, time-dependent energy gap fluctuations driven by intrinsic quantum processes—such as the polarization and vacuum fluctuations that lead to spontaneous emission and spectral diffusion—are primary sources of intrinsic noise. Intrinsic noise is often very difficult or impossible to control. By contrast, extrinsic noise can sometimes be controlled. Spin echo techniques, for example, can eliminate some extrinsic noise if it is static.¹⁴ Examples of phenomena that contribute to extrinsic noise include the statistical distribution of energy levels at finite temperatures and the distribution of orientations of molecules in a solid.

Magnetic field fluctuations are a primary source of extrinsic noise in magnetic resonance measurements.^{15–18} Several fields in quantum measurement, from ion traps to atomic clocks and molecular magnets, take advantage of avoided crossings between various spin sublevels to dampen

noise caused by fluctuating magnetic fields.^{15,18–22} At the avoided crossings with respect to the applied Zeeman field, transition frequencies become insensitive to field fluctuations because their first derivative with respect to the magnetic field vanishes. Transitions at these points are called “clock transitions,” (CTs) because of their history in atomic clocks. The dephasing “ T_2 ” times typically show a dramatic increase around the clock transitions.^{16,17,19,23–25}

Molecules, like the ones that inspire this work, have more states than atoms do. They scale better because they can keep multiple excitations coherent.²⁶ Unlike atoms in ion traps, however, molecules also have physical structure that results in more adiabatic variables. Unfortunately, the higher dimensional adiabatic manifolds in molecules are, in general, much more complex than they are in atoms. Molecular vibrations also introduce intrinsic noise in molecules that is manifestly absent in atoms. Finding CTs in molecules is much more challenging.

In this work, we study a model for a dimer undergoing singlet fission and find CTs in this higher dimensional adiabatic manifold. At the critical points that are analogous to the usual one-dimensional case, the first partial derivatives of the transition frequency with respect to *all adiabatic variables* vanishes. The CTs stabilize transitions against intrinsic and extrinsic noise.

In our analysis, fluctuating variables appear as adiabatic parameters in a model Hamiltonian, called the JDE model.⁴ It accurately predicts trEPR spectra for the two-triplet exciton pair in strongly-coupled SF dimers. Under certain conditions, the spin-polarization from the optical preparation in the trEPR experiment is high.⁴ We find a pair of CTs between the spin-polarized initial state 5TT_0 and the ${}^3TT_{-1}$ and the ${}^5TT_{+1}$ states. The critical points in the EPR transition energies emerge as a result of a conical intersection between the ${}^3TT_{-1}$ and the ${}^5TT_{+1}$ states on a periodic potential. We show the conditions under which the CTs can protect against decoherence from extrinsic *and* intrinsic noise sources, including molecular vibrations, variations in the magnetic field, and distributions in the molecular orientations.

II. METHODS

We employ the *JDE spin exciton Hamiltonian* to describe the two-triplet exciton pair in a static Zeeman field, with the triplets from the SF process localized on chromophores *A* and *B*.⁴ Following Smyser and Eaves⁴, we write the Hamiltonian in the suggestive form

$$\begin{aligned} \mathcal{H} &= H_0 + H_{ZFS}, \\ &= \mu B_0 S_z - J \vec{S}_A \cdot \vec{S}_B + \vec{S}_A^\dagger \cdot \mathbf{D}_A \cdot \vec{S}_A + \vec{S}_B^\dagger \cdot \mathbf{D}_B \cdot \vec{S}_B, \end{aligned} \tag{1}$$

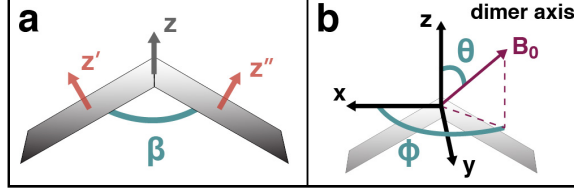


FIG. 1. Adiabatic variables include the dihedral bridging angle between two chromophores and the orientation of the magnetic field relative to the dimer. **(a)** The molecular geometry of the two chromophores (grey rectangles) joined at a bridge.^{28,29} Primed variables designate the magnetic principal axes of the individual chromophores and the unprimed ones denote the common dimer axis. **(b)** The external magnetic field B_0 is oriented to the dimer axis, given by the molecular geometry in **a**, by azimuthal ϕ and polar θ angles.

and choose units of angular momentum in terms of \hbar . The strong-field part of the Hamiltonian $H_0 = H_Z - J\vec{S}_A \cdot \vec{S}_B$ is a sum of the Dirac-Heisenberg isotropic exchange term $-J\vec{S}_A \cdot \vec{S}_B$ and the Zeeman interaction $H_Z = \mu B_0 S_Z$, where $\vec{S} = \vec{S}_A + \vec{S}_B$ is the total spin and $\mu = g\mu_B$ is the magnetic dipole moment.²⁷ The total angular momentum basis $|S, M\rangle$ diagonalizes the reference Hamiltonian H_0 and sets the quantization axis for all operators to the polarization direction of the Zeeman field—the Z axis of the lab frame. In the literature and in this manuscript, the $|S, M\rangle$ diabatic states are also labeled by $^{2S+1}TT_M$, where TT refers to the spatial nature of the spin wavefunction, the superscript denotes the state’s multiplicity in terms of its total spin quantum number S , and M is the quantum number for the projection of \vec{S} along the Z -axis. In the field-swept EPR experiment, there is an oscillating magnetic field perpendicular to Z that induces transitions between adjacent M sublevels of the same S .

The zero-field splitting term describes the triplets interacting with themselves, $H_{ZFS} = \vec{S}_A^\dagger \cdot \mathbf{D}_A \cdot \vec{S}_A + \vec{S}_B^\dagger \cdot \mathbf{D}_B \cdot \vec{S}_B$, where \mathbf{D}_A , \mathbf{D}_B are the spin-dipole tensors in the lab frame. In the principal frame of each chromophore—that need not coincide with one another or with the quantization axis of the magnetic field B_0 —the spin-dipole tensor is a traceless, diagonal matrix with matrix elements D and E . But in the lab frame, the dipole tensors are no longer diagonal and the form of H_{ZFS} is more complicated (see Appendix).

Inspired by the pioneering synthetic work in Ref. 28 and 29, we consider planar dimers connected to one another by a rigid covalent bridge that fixes their relative orientation. The angle between the chromophores is the dihedral bridging angle β (Fig. 1a), and it is the first of the adiabatic variables we consider. Molecular vibrations and structural disorder cause fluctuations in β that contribute to intrinsic and extrinsic noise, respectively. A “passive rotation” relates the

body frame, or dimer axis (x, y, z) , to the lab frame (X, Y, Z) , Fig. 1b.³⁰ The details appear in the Appendix, Eq. A.3-A.4. The orientation of the dimer frame relative to the Z -axis of the lab frame introduces two additional adiabatic variables, θ and ϕ , so that $H_{ZFS} = H_{ZFS}(\beta, \theta, \phi)$. Similar to β , these variables contribute to both extrinsic and intrinsic noise. The Hamiltonian in Eq. 1 also depends on the *local* or effective field on a molecule *in the material*. The B -field in Eq. 1 should really be understood as a local field. Local shielding effects make it a fluctuating variable in the ensemble which leads to decoherence.^{31,32} The magnetic field strength is the fourth and final adiabatic variable that we analyze in this paper, so that the total Hamiltonian depends on four adiabatic variables: β , θ , ϕ and B_0 . We use the shorthand $\Gamma = (\beta, \theta, \phi, B_0)$.

The axial and rhombic EPR parameters D and E are fixed and we choose units of energy in terms of J . For Figures 2 and 3, we use $J > 0$, $D/J = 0.1$, and $E = -D/4$. The sign $J > 0$ orders the energies of the states from highest multiplicity to lowest, in analogy with Hund’s rule for molecules, though this is not a strong rule for dimers in SF literature.²⁹ With $J > 0$, the exchange coupling orders the states in the same way as in Ref. 4. The parameter E is usually small and near zero, with the opposite sign of D .³³ A value $E = 0$, however, might lead to accidental degeneracies in the energy spectrum. Using the maximum amplitude of $|E| = |D|/3$ avoids these spurious degeneracies. But we find it also decouples the 1TT initial SF state from the rest of the $^{2S+1}TT_M$ manifold at the critical point. We instead use $E = -D/4$. These values are roughly consistent with some reported in the literature.^{6,7,9,34,35} Varying them quantitatively over several orders in magnitude does not change the qualitative results about the CTs that we report here.

III. RESULTS AND DISCUSSION

To analyze Eq. 1, it is convenient to introduce an adiabatic and a diabatic basis. The diabatic $|S, M\rangle$ states diagonalize H_0 . Their energies with respect to H_0 are only functions of B_0/J , S , and M . Because they are eigenfunctions of \vec{S}^2 and S_Z , their physical meaning is clear and they provide a convenient basis for describing state-to-state relaxation between various $^{2S+1}TT_M$ states.⁴ The adiabatic states diagonalize the full Hamiltonian in the basis of the states near the crossing and their energies depend on all four of the adiabatic variables. Because they are, generally, superpositions of the diabatic states, their physical meaning is less clear.

In the space of the adiabatic variables, away from degeneracies in H_0 , the diabatic states nearly diagonalize the Hamiltonian so that there is little difference between them and the adiabatic states.

But when diabatic states become nearly degenerate, there is an opportunity for a crossing. If the matrix element of H_{ZFS} between the diabats near the crossing is nonzero, the adiabatic states can form an *avoided crossing*. Here, the adiabatic states and energies can differ substantially from the diabats. If, however, the matrix element of H_{ZFS} between the diabats is zero, the diabats coincide with the adiabats and there is a *true crossing*. In the multidimensional adiabatic space of Eq. 1, there can be regions where the coupling vanishes only at a point, in which case the adiabatic curves form a *conical intersection*. We find examples of all three types of crossings in this manuscript.

Avoided crossings and conical intersections are the more interesting of these three crossings in this manuscript because they can give rise to clock transitions. Dipole-allowed transitions occur at frequencies Ω and are a function of the adiabatic variables, $\Omega = \Omega(\Gamma)$. A conventional one-dimensional CT occurs at critical points B_0^* , where the transition frequency is insensitive to changes in the magnetic field, $\frac{d\Omega}{dB_0}|_{B_0^*} = 0$. Similarly, in our multidimensional system, CTs occur when the transition frequency is insensitive to changes in *all of the adiabatic variables*, which happens at critical points Γ^* , where $\frac{\partial\Omega}{\partial\Gamma}|_{\Gamma^*} = 0$. For a clock transition to be relevant for quantum information, the initial state should be strongly spin-polarized.

To find a relevant CT, one has to find critical points for a dipole-allowed transition that falls within the bandwidth of the EPR measurement, *and* the initial state has to be strongly spin-polarized. These are rather strict requirements that might be met by a sophisticated search algorithm. We find them through a process of elimination. Avoided crossings in B_0 have a parabolic shape that makes them good candidates for CTs. Most of the potential crossings at B -fields relevant for X-band EPR are forbidden by dipole selection rules. Other states are very weakly coupled, such as the 1TT and $^5TT_{+2}$ states whose splitting is of order $(|E|/J)^2 \sim 10^{-4}$. Such weak coupling would be minimally stabilizing. This leaves two possible crossings; one between $^3TT_{-1}$ and $^5TT_{+1}$ and another between 3TT_0 and $^5TT_{+2}$. In this manuscript we analyze the former because the theory for the spin polarization process in the initial state is simpler. Note that this crossing would be between $^3TT_{+1}$ and $^5TT_{-1}$ for $J < 0$.

In the trEPR experiment, a laser pulse initiates the SF process which populates the singlet 1TT level.²⁹ Provided that J is large, fluctuations in J drive non-adiabatic transitions to other levels in the $^{2S+1}TT_M$ manifold.⁴ But the triangle inequality, resulting from the Wigner-Eckart theorem (Appendix Eq. A.9) forbids relaxation from the singlet 1TT state to the triplet 3TT_M levels. This has two consequences. First, all crossings between 1TT and 3TT_M are true crossings (Fig. 2a,c). Second, the relaxation from 1TT populates only the quintet 5TT_M levels with a rate

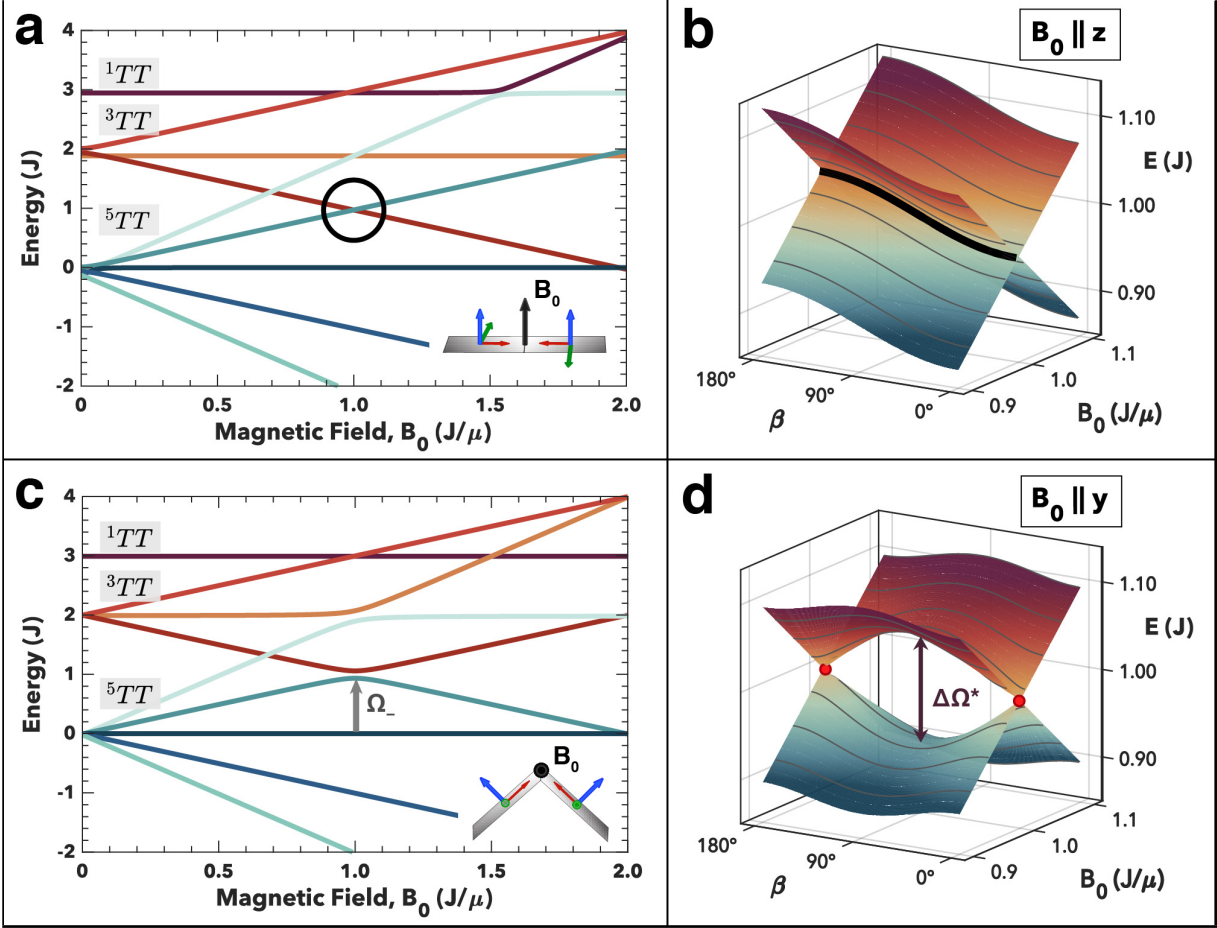


FIG. 2. The JDE Hamiltonian exhibits several potential avoided crossings, but only some are relevant to dimers in X-band EPR. The two-triplet exciton states of the singlet fission product are labeled according to their total multiplicity at strong field, $^{2S+1}TT_M$. **(a)** The field dependent energy spectrum for the all-parallel case. The black circle highlights the S, M crossing we examine in (a-d). **(b)** Upper and lower adiabatic states in the (β, B_0) plane with $B_0 \parallel z$. There is a line of true crossings (black line) on resonance, $\delta = 0$ for all β . **(c)** The field dependent energy spectrum for $B_0 \parallel y$ and $\beta = 90^\circ$. The grey arrow in (c) indicates the transition stabilized by the saddle-point in (d). **(d)** Upper and lower adiabatic states in the (β, B_0) plane with $B_0 \parallel z$ and $\beta = 90^\circ$. The coupling only disappears at a single point, where the chromophores are parallel (red points). This forms a conical intersection in the (β, B_0) plane, in contrast to the true crossings diagrammed in (b). The saddle-points in (d), indicated by the double arrow that shows the maximal splitting, $\Delta\Omega^* = \Delta\Omega(\Gamma^*)$, away from the conical intersections can stabilize the system against fluctuations in β and B_0 . The transitions corresponding to Ω_+ and Ω_- are the *clock transitions*.

proportional to $|\langle {}^1TT | H_{ZFS} | {}^5TT_M \rangle|^2$. These matrix elements determine the selection rules and the spin-polarization in the initial state. If they are large for particular values of M and small for others, the relaxation is state-specific and the quintet is strongly spin-polarized.⁴ Because H_{ZFS} depends on the adiabatic variables, the strength of the spin-polarization does too.

Smyser and Eaves⁴ showed that the “all-parallel” case of $\beta = 180^\circ$ with the magnetic field aligned along the dimer z -axis ($B_0 \parallel z$) generates strong spin-polarization in 5TT_0 . From this state, there are only a few crossings that are relevant to dimers in X-band EPR. The nearby crossing circled in Figure 2a is the only one allowed by selection rules whose transition is dipole-allowed. The transition between this state and the initial spin-polarized 5TT_0 state is a candidate CT.

The energy spectrum of the adiabats for the all-parallel case appears in Fig. 2a. Exchange symmetry demands that the couplings between the triplet and quintet levels vanish for all values of β . It follows that all crossings are true crossings in the (β, B_0) plane (Fig. 2b).⁴ Similarly, the crossing remains true for all values of ϕ and θ when $\beta = 180^\circ$. The true crossing between the quintet and triplet states precludes CTs under these conditions.

When the molecule is bent ($\beta \neq 180^\circ$) and the magnetic field is not directed along the z -axis of the chromophore pair, the intersection between ${}^3TT_{-1}$ and ${}^5TT_{+1}$ is no longer a true crossing. It now becomes a candidate for a clock transition. Near this crossing, we define the upper or lower energy branch of the adiabatic states as E_- and E_+ , respectively. Intensity borrowing from ${}^5TT_{+1}$ allows transitions from 5TT_0 to both the upper and lower branch. Shifting the reference energy so that the 5TT_0 energy is zero, the transition frequencies are $\Omega_{\pm} = E_{\pm}/(D - E)$. Ω_- is shown as a grey arrow in Fig. 2c. A useful rearrangement of Ω_{\pm} gives $\Omega_{\pm} = \bar{\Omega} \pm \Delta\Omega$, where $\bar{\Omega}$ (Eq. A.2) is a carrier frequency.

Figure 2d shows the results for the upper and lower adiabatic branches in the (β, B_0) plane for $B_0 \parallel y$. As before, the coupling vanishes when chromophores are parallel, at $\beta = 180^\circ$, but is nonzero for all other values. The upper and lower branches form a conical intersection. The periodic nature of the bridging angle imposes a boundary condition on the surfaces as they move away from the conical intersection. The lower and upper branch must have a critical point away from the conical intersection because the conical intersection pins both surfaces at the parallel $\beta = 0$ and the anti-parallel $\beta = 180^\circ$ geometries (Fig. 2d).

At the conical intersection, the transition frequency would change violently in the space of the adiabatic variables. But, away from the conical intersection, there is a pair of saddle points in the (β, B_0) plane that can stabilize a pair of transitions. As we will show, these saddle points do indeed

reflect a critical point in the full dimensional adiabatic space and correspond to clock transitions.

The transition frequencies are split by the difference $\Delta\Omega = \frac{\Omega_+ - \Omega_-}{2}$, which depends on all four adiabatic variables. It can be written in the form

$$\Delta\Omega = \sqrt{\delta^2 + \sin^2(\beta)f(\phi, \theta)}, \quad (2)$$

where

$$f(\phi, \theta) = \frac{1}{4} \sin^2(\theta) (1 - \cos^2(\phi) \sin^2(\theta)). \quad (3)$$

Candidate clock transitions occur for nonzero values of $\Delta\Omega$. More specifically, $\Delta\Omega$ is the splitting between the pair of clock transitions, which must be larger than the linewidths $\sim 1/T_2$ for the clock transitions to be resolvable. In Eq. 2, $\delta \equiv (\mu B_0 - J)/(D - E)$ is a more convenient variable than B_0 (Fig 2). But δ neatly expresses the detuning of B_0 from the avoided crossing, which occurs at resonance, $\delta = 0$ (black circle Fig. 2a). The function $f(\phi, \theta)$ is what we call *the orientor* because it completely describes the orientational dependence of the CT. In avoided crossings between two-level systems, finding the adiabatic states that diagonalize the Hamiltonian is equivalent to choosing a mixing angle that depends on two scalars. From this perspective Eq. 2 describes the transition frequency for a two-level system whose mixing angle depends on several variables δ , β , ϕ , and θ .

We find critical points of Eq. 2 analytically—it turns out that critical points in $\Delta\Omega = \Delta\Omega^*$ (double arrow Fig. 2d) are also critical points in Ω_{\pm} . At resonance, $\Delta\Omega$ is a completely separable function of the bridging angle β and the magnetic field orientations ϕ and θ . This greatly simplifies the analysis.

At resonance, the dependence on the bridging angle is a multiplicative factor of $\sin(\beta)$. This implies that a dimer with a bend of 90° would minimize extrinsic fluctuations due to orientational disorder and intrinsic fluctuations from molecular vibrations that modulate the orientations.

The orientor is a more complex function (Fig. 3). It has maxima at the critical points Γ^* when $B_0 \parallel y$, so that B_0 is aligned with the individual chromophore y' and y'' axes, which are parallel to one another for any value of β . The orientor also has a pair of saddle points at $(\phi, \theta) = (0^\circ, 45^\circ)$ and $(\phi, \theta) = (180^\circ, 45^\circ)$ that we disregard. The 5TT_0 state is weakly spin-polarized and $\Delta\Omega \sim \sqrt{f}$ is small at those saddle points compared to the maxima in f . The alignment of $B_0 \parallel y$ minimizes extrinsic sources of noise resulting from the distribution of orientation in the material as well as intrinsic noise from nuclear vibrations that modulate the orientation. Note that when $B_0 \parallel z$, the orientor is zero and the transition is not stabilized.

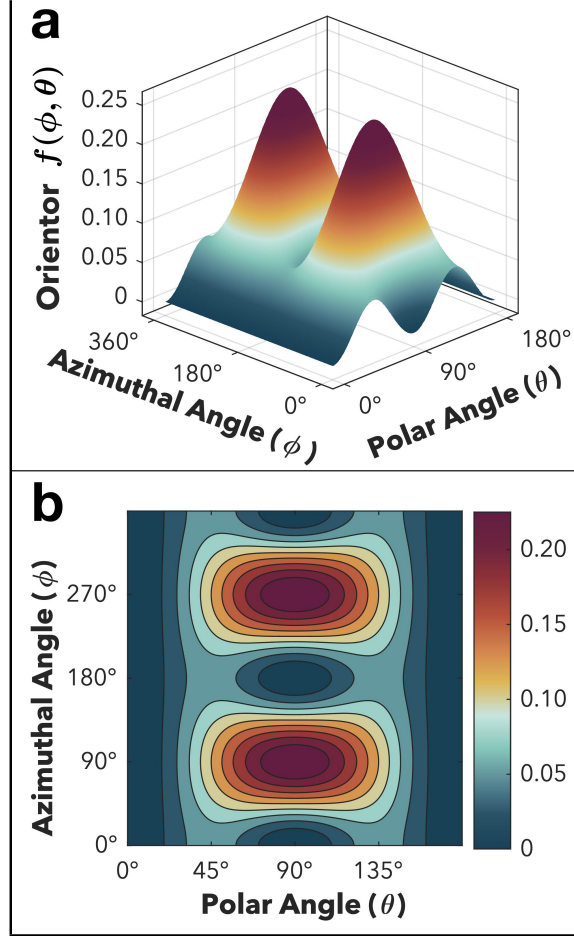


FIG. 3. The orientor function, $f(\phi, \theta)$ completely describes the orientational dependence of the splitting between upper and lower adiabatic states, given by $\Delta\Omega$ on resonance ($\delta = 0$) when the chromophores are bent ($\beta = 90^\circ$). These two adiabatic variables are set to the saddle point of Fig. 2d. (a) Surface plot and (b) contour plot of the orientor. The splitting $\Delta\Omega = \sqrt{f(\phi, \theta)}$ depends only on the orientation of the field relative to the molecular axes ϕ, θ (Fig 1b). The maxima of the orientor $f(\phi, \theta)$ are critical points that stabilize the transition frequencies against spatial fluctuations caused by static disorder or nuclear vibrations in the angles ϕ, θ of the magnetic field relative to the dimer axis.

IV. CONCLUSION

Clock transitions have a history in atomic physics literature. For quantum information applications, molecules have several advantages over atoms, but with a cost of increased complexity. We analyze the JDE model, Eq. 1,⁴ to predict a pair of clock transitions for two-triplet excitons on rigid, covalently bonded, planar dimers. Choosing the diabatic basis with respect to the lab axis

expresses the entire Hamiltonian in the stationary states of the Zeeman Hamiltonian. Away from the crossings, the zero-field Hamiltonian, while complicated in this basis, is perturbatively small. This choice of basis also provides a consistent framework for determining spin polarization in the initial states when J is large.⁴

The adiabatic eigenstates of the full Hamiltonian, as a function of the four adiabatic variables that we analyze, contain three types of crossings: avoided crossings, true crossings, and conical intersections. Under certain conditions, avoided crossings and conical intersections give rise to clock transitions. Dipole selection rules in concert with mixing rules derived from the Wigner-Eckhart theorem (see Appendix), imply that only a few crossings are relevant candidate CTs for X-band EPR.

For a relevant CT, the initial state must also be spin-polarized. We find a pair of CTs from the 5TT_0 state and the upper and lower adiabatic branches resulting from the avoided crossing between ${}^3TT_{-1}$ and ${}^5TT_{+1}$. Transitions to both branches are stabilized at the critical point $\Gamma^* = (\beta = 90^\circ, \theta = 90^\circ, \phi = 90^\circ, B_0 = J/\mu)$ —a high symmetry configuration where the magnetic field orientation $B_0 \parallel y$, aligns B_0 with the chromophore y' and y'' axes for all values of β (Fig. 2c inset).

Compared to atomic systems, molecules offer many advantages for quantum applications. Molecules, however, also have more intrinsic noise that is often difficult to control. A molecule with three dimensional structure has a non-trivial relationship between the body frame and the lab frame. The parameters that characterize this relationship introduce additional adiabatic variables that we analyze here. Internal molecular structure—in this work, the dihedral bridging angle β —introduces new adiabatic variables too. We find a pair of clock transitions for SF chromophores that, remarkably, satisfy all criteria required of a clock transition simultaneously. Clock transitions offer a rare opportunity to control intrinsic noise. We have predicted a pair of clock transitions that can extend decoherence times for two-triplet excitons on rigid, covalently bonded, planar dimers. While the molecules that we suggest have not, to our knowledge, yet been synthesized, we hope that our work inspires their creation.

AUTHOR CONTRIBUTIONS

JDE designed the research. JDE, SGL, and KES performed the research and wrote the manuscript.

ACKNOWLEDGMENTS

We thank Obadiah Reid and Brandon Rugg for introducing us to the topic of clock transitions. Funding was provided by the United States Department of Energy, Office of Basic Energy Sciences (ERW7404).

COMPETING INTERESTS

The authors declare no competing interests.

DATA AVAILABILITY STATEMENT

The data that support the findings of this study are available from the corresponding author upon reasonable request.

Appendix A: Appendix A: Selection Rules of the JDE Model

The reference Hamiltonian is diagonal in the diabatic basis discussed in the text

$$\langle S', M' | H_0 | S, M \rangle = \left(\mu B_0 M - \frac{J}{2} (S(S+1) - 4) \right) \delta_{S'=S} \delta_{M'=M}. \quad (\text{A.1})$$

Eq. 1 is written in the lab frame. Solving for the matrix elements of the zero-field splitting Hamiltonian requires relating the spin-dipole tensor in the principal frame, where the parameters D and E are known, to its representation in the lab frame. In the principal frame of chromophore i the spin-dipole tensor D''_i is symmetric and traceless

$$D''_A = D''_B = \begin{pmatrix} -D/3 + E & 0 & 0 \\ 0 & -D/3 - E & 0 \\ 0 & 0 & 2D/3 \end{pmatrix}. \quad (\text{A.2})$$

We relate the principal frame of the two chromophores to the lab frame by a series of rotations. First, the molecules are symmetrically rotated via an active rotation $R_A(\pm\Theta_\beta)$ to obtain the desired bridging angle β of the dimer as shown in Fig. 1a. Second, a passive rotation $R_P(\Theta_B)$ is applied to both chromophores to describe the orientation of the applied magnetic field with respect to the

shared dimer axis.

$$D_A = R_P(\Theta_B) R_A(-\Theta_\beta) D_A'' R_A^{-1}(-\Theta_\beta) R_P^{-1}(\Theta_B), \quad (\text{A.3})$$

$$D_B = R_P(\Theta_B) R_A(\Theta_\beta) D_B'' R_A^{-1}(\Theta_\beta) R_P^{-1}(\Theta_B). \quad (\text{A.4})$$

Following the method outlined in Mueller³⁰, we write the matrix elements of H_{ZFS} as

$$\begin{aligned} \langle S' M' | H_{ZFS} | S M \rangle &= \sum_{i,j,k=-2}^2 (-1)^{k-M'} \sqrt{5(2S+1)(2S'+1)} D_i^{(2)} \left(\mathcal{D}_{kj}^{(2)}(\Theta_B) \right)^\dagger \\ &\times \begin{pmatrix} 2 & S & S' \\ -k & M & -M' \end{pmatrix} \begin{Bmatrix} 1 & 1 & 2 \\ S' & S & 1 \end{Bmatrix} \left(\mathcal{D}_{ji}^{(2)}(\Theta_\beta) + (-1)^{S'+S} \mathcal{D}_{ji}^{(2)}(-\Theta_\beta) \right), \end{aligned} \quad (\text{A.5})$$

where $D_i^{(2)}$ is the i th component of the 2nd rank spherical tensor representation of the ZFS tensor D in the principal frame (e.g. $D_0^{(2)} = \sqrt{2/3}D$, $D_{\pm 1}^{(2)} = 0$, $D_{\pm 2}^{(2)} = E$) and $\mathcal{D}_{i,j}^{(2)}(\Theta)$ are the Wigner rotation matrix elements for a rotation defined by the set of angles Θ . We use the typical physics convention to define the Wigner rotation matrix elements. The Wigner-3j symbol is best defined in relation to Clebsch-Gordon coefficients for adding angular momentum j_1 and j_2 to get j_3 ,

$$\begin{pmatrix} j_1 & j_2 & j_3 \\ m_1 & m_2 & m_3 \end{pmatrix} = \frac{(-1)^{j_2-j_1+m_3}}{\sqrt{2j_3+1}} \langle j_1, m_1; j_2, m_2 | j_1, j_2; j_3, -m_3 \rangle. \quad (\text{A.6})$$

The Wigner-6j symbol is a sum over Wigner-3j symbols,

$$\begin{aligned} \begin{Bmatrix} j_1 & j_2 & j_3 \\ j_4 & j_5 & j_6 \end{Bmatrix} &= \sum_{m_i} (-1)^{\sum_k (j_k - m_k)} \begin{pmatrix} j_1 & j_2 & j_3 \\ -m_1 & -m_2 & -m_3 \end{pmatrix} \\ &\times \begin{pmatrix} j_1 & j_5 & j_6 \\ m_1 & -m_5 & -m_6 \end{pmatrix} \begin{pmatrix} j_4 & j_2 & j_6 \\ m_4 & m_2 & -m_6 \end{pmatrix} \begin{pmatrix} j_4 & j_5 & j_3 \\ -m_4 & m_5 & m_3 \end{pmatrix}. \end{aligned} \quad (\text{A.7})$$

The orthogonality properties of the Wigner-3j and Wigner-6j symbols provide the selection rules for transitions between $|S', M'\rangle$ and $|S, M\rangle$

$$S' + S \geq 2, \quad (\text{A.8})$$

$$|S - 2| \leq S' \leq S + 2, \quad (\text{A.9})$$

$$M - M' = k, \quad (\text{A.10})$$

where k is an integer between -2 and 2 . Eq. A.8 follows from the Wigner-6j triangle inequality $|j_4 - j_5| \leq j_3 \leq j_4 + j_5$. Eq. A.9, which follows from the Wigner-3j triangle inequality, can be

shown to give the same restriction. We note that for parallel chromophores, where $\mathcal{D}_{ji}^{(2)}(\theta_\beta) = \mathcal{D}_{ji}^{(2)}(-\theta_\beta)$, we require the additional condition $S' + S$ is even. For parallel chromophores, the coupling matrix elements between 3TT and 1TT , 5TT are strictly zero.

Appendix B: Appendix B: Transition Frequency between Quintet $M = 0$ and Upper/Lower Adiabatic Branch

With the reference energy set so that the 5TT_0 energy is zero, the transition frequency to the adiabatic states considered in the main text $\Omega_\pm = E_\pm/(D - E)$ is

$$\Omega_\pm = \bar{\Omega} \pm \Delta\Omega, \quad (\text{A.1})$$

where

$$\begin{aligned} \bar{\Omega} = 1 + \frac{(D+3E)}{12}(1 - 3\sin^2\theta\sin^2\phi) \\ + \frac{(D-E)}{4}\cos\beta(\sin^2\theta(1 + \cos^2\phi) - 1), \end{aligned} \quad (\text{A.2})$$

$$\Delta\Omega = \sqrt{\delta^2 + \sin^2(\beta)f(\phi, \theta)}, \quad (\text{A.3})$$

$$f(\phi, \theta) = \frac{1}{4}\sin^2(\theta)(1 - \cos^2(\phi)\sin^2(\theta)), \quad (\text{A.4})$$

and $\delta = (\mu B_0 - J)/(D - E)$.

REFERENCES

- ¹M. B. Smith and J. Michl, ‘‘Singlet Fission,’’ *Chemical Reviews* **110**, 6891–6936 (2010).
- ²M. B. Smith and J. Michl, ‘‘Recent Advances in Singlet Fission,’’ *Annual Review of Physical Chemistry* **64**, 361–386 (2013).
- ³M. C. Hanna and A. J. Nozik, ‘‘Solar conversion efficiency of photovoltaic and photoelectrolysis cells with carrier multiplication absorbers,’’ *Journal of Applied Physics* **100**, 074510 (2006).
- ⁴K. E. Smyser and J. D. Eaves, ‘‘Singlet fission for quantum information and quantum computing: the parallel JDE model,’’ *Scientific Reports* **10**, 18480 (2020).
- ⁵G. Tao, ‘‘Topology of quantum coherence in singlet fission: Mapping out spin micro-states in quasi-classical nonadiabatic simulations,’’ *The Journal of Chemical Physics* **152**, 074305 (2020).

- ⁶L. R. Weiss, S. L. Bayliss, F. Kraffert, K. J. Thorley, J. E. Anthony, R. Bittl, R. H. Friend, A. Rao, N. C. Greenham, and J. Behrends, “Strongly exchange-coupled triplet pairs in an organic semiconductor,” *Nature Physics* **13**, 176–181 (2017).
- ⁷M. J. Y. Tayebjee, S. N. Sanders, E. Kumarasamy, L. M. Campos, M. Y. Sfeir, and D. R. McCamey, “Quintet multiexciton dynamics in singlet fission,” *Nature Physics* **13**, 182–188 (2017).
- ⁸A. K. Le, J. A. Bender, D. H. Arias, D. E. Cotton, J. C. Johnson, and S. T. Roberts, “Singlet Fission Involves an Interplay between Energetic Driving Force and Electronic Coupling in Perylenediimide Films,” *Journal of the American Chemical Society* **140**, 814–826 (2018).
- ⁹D. Lubert-Perquel, E. Salvadori, M. Dyson, P. N. Stavrinou, R. Montis, H. Nagashima, Y. Kobori, S. Heutz, and C. W. M. Kay, “Identifying triplet pathways in dilute pentacene films,” *Nature Communications* **9**, 4222 (2018).
- ¹⁰M. Chen, M. D. Krzyaniak, J. N. Nelson, Y. J. Bae, S. M. Harvey, R. D. Schaller, R. M. Young, and M. R. Wasielewski, “Quintet-triplet mixing determines the fate of the multiexciton state produced by singlet fission in a terrylenediimide dimer at room temperature,” *Proceedings of the National Academy of Sciences of the United States of America* **116**, 8178–8183 (2019).
- ¹¹W. S. Warren, “The Usefulness of NMR Quantum Computing,” *Science* **277**, 1688–1690 (1997).
- ¹²D. P. DiVincenzo, “The Physical Implementation of Quantum Computation,” *Fortschritte der Physik* **48**, 771–783 (2000).
- ¹³N. G. V. Kampen, *Stochastic Processes in Physics and Chemistry* (North Holland, 2007).
- ¹⁴E. L. Hahn, “Spin echoes,” *Phys. Rev.* **80**, 580–594 (1950).
- ¹⁵T. Rosenband, D. B. Hume, P. O. Schmidt, C. W. Chou, A. Brusch, L. Lorini, W. H. Oskay, R. E. Drullinger, T. M. Fortier, J. E. Stalnaker, S. A. Diddams, W. C. Swann, N. R. Newbury, W. M. Itano, D. J. Wineland, and J. C. Bergquist, “Frequency Ratio of Al⁺ and Hg⁺ Single-Ion Optical Clocks; Metrology at the 17th Decimal Place,” *Science* **319**, 1808–1812 (2008).
- ¹⁶H. Seo, A. L. Falk, P. V. Klimov, K. C. Miao, G. Galli, and D. D. Awschalom, “Quantum decoherence dynamics of divacancy spins in silicon carbide,” *Nature Communications* **7**, 12935 (2016).
- ¹⁷K. C. Miao, J. P. Blanton, C. P. Anderson, A. Bourassa, A. L. Crook, G. Wolfowicz, H. Abe, T. Ohshima, and D. D. Awschalom, “Universal coherence protection in a solid-state spin qubit,” *Science* **369**, 1493–1497 (2020).
- ¹⁸M. Rubín-Osanz, F. Lambert, F. Shao, E. Rivière, R. Guillot, N. Suaud, N. Guihéry, D. Zueco, A.-L. Barra, T. Mallah, and F. Luis, “Chemical tuning of spin clock transitions in molecular

- monomers based on nuclear spin-free Ni(ii),” *Chemical Science* **12**, 5123–5133 (2021).
- ¹⁹C. Langer, R. Ozeri, J. D. Jost, J. Chiaverini, B. DeMarco, A. Ben-Kish, R. B. Blakestad, J. Britton, D. B. Hume, W. M. Itano, D. Leibfried, R. Reichle, T. Rosenband, T. Schaetz, P. O. Schmidt, and D. J. Wineland, “Long-Lived Qubit Memory Using Atomic Ions,” *Physical Review Letters* **95**, 060502 (2005).
- ²⁰C. A. Collett, P. Santini, S. Carretta, and J. R. Friedman, “Constructing clock-transition-based two-qubit gates from dimers of molecular nanomagnets,” *Physical Review Research* **2**, 032037 (2020).
- ²¹S. Giménez-Santamarina, S. Cardona-Serra, J. M. Clemente-Juan, A. Gaita-Ariño, and E. Coronado, “Exploiting clock transitions for the chemical design of resilient molecular spin qubits,” *Chemical Science* **11**, 10718–10728 (2020).
- ²²J. Chen, C. Hu, J. F. Stanton, S. Hill, H.-P. Cheng, and X.-G. Zhang, “Decoherence in Molecular Electron Spin Qubits: Insights from Quantum Many-Body Simulations,” *The Journal of Physical Chemistry Letters* **11**, 2074–2078 (2020).
- ²³H. Katori, M. Takamoto, V. G. Pal’chikov, and V. D. Ovsiannikov, “Ultrastable Optical Clock with Neutral Atoms in an Engineered Light Shift Trap,” *Physical Review Letters* **91**, 173005 (2003).
- ²⁴K. Beloy, A. Derevianko, V. A. Dzuba, and V. V. Flambaum, “Micromagic Clock: Microwave Clock Based on Atoms in an Engineered Optical Lattice,” *Physical Review Letters* **102**, 120801 (2009).
- ²⁵M. Shiddiq, D. Komijani, Y. Duan, A. Gaita-Ariño, E. Coronado, and S. Hill, “Enhancing coherence in molecular spin qubits via atomic clock transitions,” *Nature* **531**, 348–351 (2016).
- ²⁶L. M. K. Vandersypen, M. Steffen, G. Breyta, C. S. Yannoni, M. H. Sherwood, and I. L. Chuang, “Experimental realization of Shor’s quantum factoring algorithm using nuclear magnetic resonance,” *Nature* **414**, 883–887 (2001).
- ²⁷J. A. Weil and J. R. Bolton, *Electron Paramagnetic Resonance: Elementary Theory and Practical Applications, Second Edition* (John Wiley and Sons, Inc, 2006).
- ²⁸T. J. Carey, E. G. Miller, A. T. Gilligan, T. Sammakia, and N. H. Damrauer, “Modular Synthesis of Rigid Polyacene Dimers for Singlet Fission,” *Organic Letters* **20**, 457–460 (2018).
- ²⁹A. T. Gilligan, E. G. Miller, T. Sammakia, and N. H. Damrauer, “Using Structurally Well-Defined Norbornyl-Bridged Acene Dimers to Map a Mechanistic Landscape for Correlated Triplet Formation in Singlet Fission,” *Journal of the American Chemical Society* **141**, 5961–

- 5971 (2019).
- ³⁰L. J. Mueller, “Tensors and rotations in NMR,” *Concepts in Magnetic Resonance Part A* **38A**, 221–235 (2011).
- ³¹R. Kubo and N. Hashitsume, “Brownian Motion of Spins,” *Progress of Theoretical Physics Supplement* **46**, 210–220 (1970).
- ³²K. Miyazaki and K. Seki, “Brownian motion of spins revisited,” *The Journal of Chemical Physics* **108**, 7052–7059 (1998).
- ³³C. E. Swenberg and N. E. Geacintov, “Exciton interactions in organic solids,” in *Organic molecular photophysics*, Vol. 1 (Wiley, London, 1973) pp. 489–564.
- ³⁴H. Sternlicht and H. M. McConnell, “Paramagnetic Excitons in Molecular Crystals,” *The Journal of Chemical Physics* **35**, 1793–1800 (1961).
- ³⁵L. Yarnus, J. Rosenthal, and M. Chopp, “EPR of triplet excitations in tetracene crystals: spin polarization and the role of singlet exciton fission,” *Chemical Physics Letters* **16**, 477–481 (1972).